Model Neural Prostheses With Integrated Microfluidics: A Potential Intervention Strategy for Controlling Reactive Cell and Tissue Responses

Scott T. Retterer*, Karen L. Smith, Christopher S. Bjornsson, Keith B. Neeves, Andrew J. H. Spence, James N. Turner, William Shain, and Michael S. Isaacson, *Member, IEEE*

***Abstract*—Model silicon intracortical probes with microfluidic channels were fabricated and tested to examine the feasibility of using diffusion-mediated delivery to deliver therapeutic agents into the volume of tissue exhibiting reactive responses to implanted devices. Three-dimensional probe structures with microfluidic channels were fabricated using surface micromachining and deep reactive ion etching (DRIE) techniques. *In vitro* functional tests of devices were performed using fluorescence microscopy to record the transient release of Texas Red labeled transferrin (TR-transferrin) and dextran (TR-dextran) from the microchannels into 1% w/v agarose gel. *In vivo* performance was characterized by inserting devices loaded with TR-transferrin into the premotor cortex of adult male rats. Brain sections were imaged using confocal microscopy. Diffusion of TR-transferrin into the extracellular space and uptake by cells up to 400 μm from the implantation site was observed in brain slices taken 1 h postinsertion. The reactive tissue volume, as indicated by the presence of phosphorylated mitogen-activated protein kinases (MAPKs), was characterized using immunohistochemistry and confocal microscopy. The reactive tissue volume extended 600, 800, and 400 μm radially from the implantation site at 1 h, 24 h, and 6 weeks following insertion, respectively. These results indicate that diffusion-mediated delivery can be part of an effective intervention strategy for the treatment of reactive tissue responses around chronically implanted intracortical probes.**

***Index Terms*—Biocompatibility, drug delivery, microfluidics, neural prostheses, reactive response.**

Manuscript received October 31, 2003; revised March 21, 2004. This work was supported in part by the National Institutes of Health and by the National Institute of Biomedical Imaging and Bioengineering under Grant EB-000359. This work was supported by funds from an NIH/NINDS grant; Neural Prostheses: Tissue Compatibility and Integration, NIH/NINDS 9R01NS-40977-05. *Asterisk indicates corresponding author.*

*S. T. Retterer is in the Biomedical Engineering Program at Cornell University, Ithaca, NY 14853 USA (e-mail: str8@cornell.edu).

K. L. Smith and C. S. Bjornsson are with the Wadsworth Center, Albany, NY 12201-0509 USA (e-mail: klsmith@wadsworth.org: cbjornss@wadsworth.org).

K. B. Neeves is with the School of Chemical and Biomolecular Engineering at Cornell University, Ithaca, NY 14853 USA (e-mail: kbn4@cornell.edu).

A. J. H. Spence was with the School of Applied and Engineering Physics at Cornell University, Ithaca, NY 14853 USA. He is now with the Department of Environmental Sciences, University of California Berkeley, Berkeley, CA 97404 USA (e-mail: aspence@nature.berkeley.edu).

J. N. Turner and W. Shain are with the Wadsworth Center, Albany, NY 12201-0509 USA and also with the Department of Biomedical Sciences, School of Public Health, State University of New York, Albany NY 12201-0509 USA (e-mail: turner@wadsworth.org; shain@wadsworth.org).

M. S. Isaacson is with the Department of Electrical Engineering, University of California at Santa Cruz, Santa Cruz, CA 95064 USA (e-mail: msi@soe.ucsc.edu).

Digital Object Identifier 10.1109/TBME.2004.834288

I. Introduction

TECHNOLOGIES aimed at extracting information directly from the brain are a key component in prosthetic systems intended to restore sensory or motor function to patients suffering from the breakdown of normal signaling pathways. Establishing a stable brain-computer interface (BCI) provides an alternative signal pathway that allows activity from the brain to be recorded, processed, analyzed and used to control complex prosthetic and communication systems [1].

Current BCI technology relies primarily on information obtained from field potentials recorded using surface electroencephalogram (EEG) to direct basic control tasks. It has been proposed, however, that information could be gathered with higher transfer rates (bit rates) and better spatial resolution by using implantable multielectrode arrays to record local-field potentials from single neurons in the cortex. However, despite the potential improvements in BCI technology, the use of intracortical probes has been hindered by a general lack of functional stability during chronic use. The primary contributors to this instability are the cell and tissue reactive responses that occur around implanted devices. Consequently developing a thorough understanding of these responses and implementing intervention strategies to promote long-term stability is critical to the development of implantable BCI technology.

Neural probes are capable of transducing cortical activity in the form of local-field potentials into electrical signals that can be conditioned, transmitted, and utilized to drive complex systems. Silicon-based cortical probes, such as those pioneered at the University of Michigan and University of Utah have gained acceptance in the neuroscience community and have been used to acutely monitor cortical activity in behaving animals [2]–[4]. Alternative silicon-based cortical probes, as well as probes made from materials such as polyimide, and other ceramics [5]–[7] have also been developed; however, their general use and characterization has been limited.

Though intracortical probes have gained acceptance as useful tools for acute behavioral studies, their chronic use has been limited by their unpredictable failure over extended periods. Some users have reported success rates in animals as high as 83% of implanted electrodes functioning with at least 63% active recording sites beyond 6 weeks [8], but it is clear that devices to be used in human prostheses must be 100% functional for the entire lifetime of the patient. Therefore, it is essential that the mechanisms contributing to the loss of device functionality be

elucidated and that strategies for stabilizing chronic devices be developed.

It has been proposed, that the primary causes of this functional failure are the reactive cell and tissue responses. These responses are characterized by the formation of a dense cellular sheath around the implanted electrode arrays [9]–[12], which results in dramatic increases in device impedance. This increase in impedance makes accurate recording of low-level signals nearly impossible. It appears that it is this characteristic change at the device/tissue interface that causes the loss of device functionality.

Pharmacological intervention via systemic injections or slow release of anti-inflammatory agents from polymers has been shown to alter the cell and tissue responses around implanted devices [12], [13]. Systemic injection, though effective and relatively easy to implement over the short term, is not a viable option for chronic intervention because of the side effects associated with long-term use of anti-inflammatory drugs. These side effects will not be present when using local delivery strategies. Additionally, local delivery strategies reduce the amount of material required, eliminate the possibility of peripheral metabolism, circumvent the blood-brain barrier, and provide immediate access to the target tissue/cells. Microchannel networks integrated into cortical probes provide an active pathway for local drug delivery that could facilitate the suppression of reactive responses and the promotion of device functional stability by altering the chemical environment in the reactive tissue around the implanted electrode array.

This paper describes the fabrication of a model silicon intracortical probe with integrated microfluidic channels for local drug delivery, and examines the feasibility of using diffusion mediated transport to deliver therapeutics throughout the entire reactive tissue volume. Immunohistochemical methods used to map the reactive tissue volume are described. These results are compared with *in vitro* and *in vivo* tests performed to demonstrate device function. Results are used to discuss the feasibility and theoretical basis for microfluidic drug delivery systems used to affect the chemical composition of the reactive tissue volume. A brief description of the reactive response and analytical models for predicting diffusion in brain tissue are also provided.

II. Reactive Cell and Tissue Responses

Reactive cell and tissue responses can be described as having two stages [6]. The intensity of the first stage, or early response, is proportional to the amount of tissue damage caused during the insertion of the multielectrode array [10]. Insertion techniques and device size can be altered to minimize trauma. However, the dense vasculature network throughout the brain makes disruption of the blood brain barrier during insertion unavoidable, resulting in the activation of inflammatory components of the early response. Immediate and transient changes in the activation of several mitogen-activated protein kinases (MAPKs), a family of enzymes that participate in intracellular signal-transduction, are characteristic of the early reactive responses [14]. By mapping the activation of two closely related MAPKs, stress-activated protein kinase/c-Jun NH2-terminal kinase (SAPK/JNK), following implantation, it is possible to determine the size of the tissue volume that recognizes and reacts to the presence of an implanted device. Local delivery of pharmacological agent(s) capable of attenuating the inflammatory signals associated with the disruption of the blood brain barrier immediately following insertion may be the first step in an intervention strategy for limiting or suppressing the early response.

In contrast to the early response, the intensity of the sustained response is independent of the amount of trauma caused during insertion and is characterized by the formation of an encapsulating cellular sheath. [9], [10]. This response is relatively independent of probe size and insertion method. The compact sheath formed during the sustained response contains microglia, astrocytes, vasculature, and extracellular proteins. As previously mentioned, this sheath contributes to decreases in electrode performance by forming an insulating sheath around the implanted electrodes. An intervention strategy consisting of both an early dose and sustained delivery of pharmacological agents should limit or disrupt the formation of the encapsulating cellular sheath, thus improving the long-term efficiency of chronically implanted electrode arrays.

III. Fluid Delivery in Neural Tissue

Local fluidic delivery of molecules in neural tissue is a complex problem requiring a thorough understanding of a host of transport and metabolic processes. Molecular diffusivity, tissue permeability, drug receptor density, drug solubility, and osmotic pressure are only a few of the factors that could potentially alter the distribution of locally delivered therapeutics *in vivo*. This complexity suggests that experimental examination of delivery *in vivo* is necessary in order to develop a better understanding of the problem and provide data for the verification of complex finite element models.

Recent efforts in the development of cortical probe technologies have focused on the design and integration of microfluidic drug delivery systems into functioning electrical devices. These devices afford the researcher the ability to induce changes in the local chemical environment surrounding the implanted device, facilitating the stimulation or suppression of acute neural activity. Successful integration of microfluidic channels capable of delivering controlled volumes of neuromodulators has been demonstrated and used to alter acute neural activity during recordings [15], [16]. Additionally, the integration of microfluidic components such as pumps and passive valves has been described [17]. However, the effectiveness of such components for accurately controlling delivery *in vivo* has yet to be shown.

Control of fluid flow with high temporal and volumetric resolution is necessary for altering and studying neuron function. Rapid inactivation and desensitization of neural responses requires precise control. However, in this paper, we examine the potential effectiveness of diffusion-driven drug delivery as a means of directing or intervening in cellular events that occur on a longer time scale. Events associated with the reactive responses may be chronically activated and develop over the course of a few hours, days, or weeks. Thus, it may be necessary

to develop and maintain therapeutic levels of a particular agent over extended periods, making high temporal and volumetric resolution unnecessary.

Both convective and diffusion-mediated transport, can be used to deliver material into the local tissue environment. Convective delivery utilizes controlled increases in pressure to drive material into the extracellular space. Pressure can be applied continuously or in controlled bursts to maintain control over local material concentrations. This approach offers a significant degree of versatility and facilitates potential control over the chemical composition of tissue up to millimeters away from the insertion site. The primary drawback to such an approach lies in its complexity and the possibility of activating biological events due to transient osmotic and/or pressure changes. In order to achieve accurate control of local concentrations, moving parts such as valves, flow meters and pumps need to be integrated into device designs. These moving parts represent possible areas of weakness in device durability. They may also require additional power and control signals that surpass the capacity of current radio frequency telemetric technology or interfere with neural signals. Alternatively they may require physical connections to outside devices that potentially degrade the mechanical stability of implanted devices.

Diffusion mediated transport on the other hand, utilizes concentration gradients established between the device reservoir and surrounding tissue environment to transport material into the extracellular space. The affected tissue volume is typically on the order of hundreds of micrometers depending on factors previously mentioned, and is, therefore, smaller than the tissue volume affected during convective delivery. Though diffusion-mediated transport does not offer the same control that convective delivery offers, it provides a simple alternative that eliminates the need for integrated moving parts, external control systems and power supplies. As previously mentioned, reactive responses take place over extended time periods. Therefore, intervention does not require rapid application of bursts of drugs, but rather the long-term maintenance of therapeutic drug concentrations. Thus, while not useful for initiation of neuronal events, we expect diffusion-mediated drug delivery to be ideal for controlling reactive responses. This work examines the feasibility of relying on diffusion to alter the chemical composition of the tissue volume exhibiting reactive responses around an implanted model silicon cortical probe.

IV. Analytical Modeling of Diffusion From Microchannels

Predictions of local drug concentrations and distribution profiles can be made using relatively simple analytical models to examine diffusion mediated delivery in the brain. Care must be taken to avoid overstating the accuracy of these models because of the complex nature of molecular transport in the brain and the complicated geometry of the delivery systems of interest. However, it is reasonable to use these models to predict the drug distribution profile within a given range for reasonable values of the apparent diffusivity, $\mathbf{D}^*$, and first-order elimination constant, $\mathbf{k}^*$, for a given molecule. An in-depth description of analytical models used to examine the diffusion of drugs from slow release polymers is given elsewhere [18], but a brief summary is given here.

The general equation for transport near a source in the brain is given as

$$\frac{\partial C}{\partial t} + v \bullet \nabla C = D_b \nabla^2 C + R_e(C) - \frac{\partial B}{\partial t}. \tag{1}$$

C is the concentration of the molecule in tissue ($\mathrm{g/cm^3}$ tissue), v is the fluid velocity (cm/s), D_b is the diffusion coefficient ($\mathrm{cm^2/s}$) of the molecule in a tissue of tortuosity, τ, $R_e(C)$ is the rate of elimination of drug ($\mathrm{g/cm^3 s}$) from the extra cellular fluid, and B is the concentration of drug bound or internalized in cells ($\mathrm{g/cm^3}$)

$$D_b = \frac{D_{\mathrm{ecf}}}{\tau}. \tag{2}$$

D_{ecf} is the diffusivity of the molecule in the extracellular fluid. For the case of strictly diffusion mediated transport, $v = 0$, and the corresponding term in the above equation can be dropped. B is assumed to be proportional to the concentration of the molecule in the tissue with proportionality constant K_{bind}. Assuming that the rate of elimination of molecules from the tissue due to enzymatic transformation, nonenzymatic elimination, and transport through the blood brain barrier, can be modeled as a first-order reaction with a reaction constant k_{app}, (1) can be expressed as

$$\frac{\partial C}{\partial t} = \frac{1}{1 + K_{\mathrm{bind}}} \left[D_b \nabla^2 C - k_{\mathrm{app}} C \right] \tag{3}$$

and simpflified further to give

$$\frac{\partial C}{\partial t} = D^* \nabla^2 C - k^* C \tag{4}$$

where $D^* = D_b/(1 + K_{\mathrm{bind}})$ and $k^* = k_{\mathrm{app}}/(1 + K_{\mathrm{bind}})$.

Applying the appropriate boundary conditions and assuming no elimination, (4) can be solved in spherical coordinates to yield

$$\frac{C}{C_0} = \frac{a}{r} erfc\left(\frac{r-a}{2\sqrt{Dt}}\right)$$

where

$$\begin{aligned} C(r=0,t) &= C_0 \\ C(r=\infty,t) &= 0 \\ C(r,t=0) &= 0 \\ r > a, \quad t &> 0. \end{aligned} \tag{5}$$

Accounting for elimination, the steady-state solution for the same boundary conditions is given as

$$\frac{C(r,t)}{C_0} = \frac{a}{r} \exp\left(-\phi\left(\frac{r}{a} - 1\right)\right)$$

where

$$\phi = \frac{k^* a^2}{D^*}. \tag{6}$$

a is the radius of a spherical source and r is the radial distance from the center of the source to some point outside of the source. For $(r - a) \ll a$, (5) and (6) will resemble the one-dimensional rectangular coordinate solution of (4). a determines

the sensitivity of the solution to three-dimensional (3-D) diffusion. For the practical application of the model to a 3-D system with a nonspherical source (i.e., multiple ports along a microfluidic channel) some appropriate value for a must be used. In this study $a = 500$ μm was used to compare measured fluorescence distributions with theoretical solutions. This choice of $a = 500$ μm compensates for the effects of diffusion in all possible radial directions. It should be noted that the distributions predicted by (5) and (6) are sensitive to choices for a, k^* and D^*. Therefore it is essential that future work focus on the development of methods for determining these parameters for various molecules and system geometries.

V. Materials and Methods

A. Device Design and Fabrication

First-generation model probes were fabricated using conventional lithographic and deep reactive ion etching (DRIE) techniques. These probes are described elsewhere and have been used in previous biocompatibility studies to stimulate the cellular and tissue reactive responses in adult rat brain tissue [9], [10], [12]–[14]. These devices were used in the current study to stimulate cellular and tissue reactive responses during the MAPK assays designed to determine the extent of the reactive tissue volume. The model probes have a shank that is 2 mm long with a 100 μm $\times$ 100 μm cross section. The device handle, or tab, used to grip probes during alignment and insertion is a cube with a side length of 500 μm. This feature allow the probes to be gripped by an automated inserter [9], [10] that helps to insure that each insertion is similar. This reduces the variability in the biological responses that can be correlated with device orientation, insertion speed, and movement.

Second-generation model cortical implants with fluid channels were fabricated by integrating the deep etching techniques utilized for the fabrication of the first-generation model probes with surface micromachining techniques previously used in the fabrication of vacuum-sealed microlamps, and silicon microneedles [19], [20]. This integrated technique allows for the fabrication of highly adaptable 3-D structures with integrated fluidic microchannels. The process is CMOS compatible and amenable to the addition of metal thin-film electrodes for recording and stimulating neural activity.

Fabrication begins by using plasma enhanced chemical vapor deposition (PECVD) and reactive ion etching (RIE) to deposit and pattern two layers of silicon dioxide on 100–mm-diameter $\langle 100 \rangle$ silicon substrates. These layers define the inner hydraulic diameter of the fluid channels [Fig. 1(a)]. The thickness of the first layer is typically 2500 nm, but can be varied to change the height of the channel cross section. The second silicon dioxide layer is approximately 500 nm thick and is aligned and patterned on top of the first layer to complete the formation of the inner, sacrificial, portion of the channel. The resulting channel cross section is a "step" with a total width of 40 μm and a center step height of 3 μm, spanning a width of 25 μm. The thinner sides of the channel are 500 nm thick. This "step" cross section allows etch vias required for the removal of the sacrificial layer to be sealed without blocking the entire channel [Fig. 1(e)].

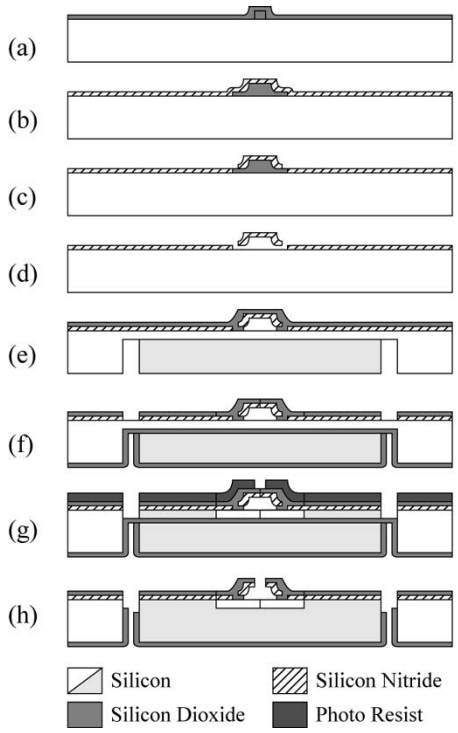

Fig. 1. (a) Two PECVD SiO_2 layers are patterned to form the inner hydraulic diameter of the channels, (b) low-stress LPCVD silicon nitride is deposited, (c) via holes are opened, and (d) the sacrificial silicon dioxide is removed. (e) Vias are sealed with a 2-μm layer of silicon dioxide. DRIE is used to etch the backside of the wafer. (f) RIE is performed to pattern the frontside hard mask, and a silicon dioxide etch stop is deposited on the backside of the wafer. (g) The final photoresist etch mask is aligned and patterned and the DRIE etching is completed. (h) A final RIE and oxygen plasma cleaning complete the process.

Throughout the fabrication process conventional contact photolithography was used to pattern photoresist etch masks for RIE processing.

The structural wall of the channel is formed using low-pressure chemical vapor deposition (LPCVD) to deposit a low-stress silicon nitride film on the silicon dioxide sacrificial layer. This silicon-rich film has a tensile stress of approximately 200 MPa, roughly five times less than standard silicon nitride films, making it less susceptible to cracking or collapse resulting from residual film stress. Following the deposition of the structural silicon nitride film, 6 μm $\times$ 10 μm via holes are etched, using an RIE process, into the silicon nitride along the thinner, 500 μm thick, portion of the channel [Fig. 1(d)]. The samples are then placed in 49% hydrofluoric acid until the sacrificial oxide is completely removed. The etch vias are sealed by depositing a 2-μm-thick PECVD silicon dioxide film. This film is later patterned and used as a hard etch mask for DRIE processing.

Once the microchannels are formed, the backside of the wafer is patterned to form the handle of the device and define the thickness of the device shank. The wafer is masked with 10 μm of photoresist. Exposed silicon is then etched using a DRIE tool (Unaxis USA inc., St. Petersburg, FL) running a standard Bosch etch process [21]. The etch depth, and the wafer thickness determine the final dimensions of the device shank. The wafer is typically etched until only 100 μm of silicon remains. However,

because the process does not rely on an etch stop, devices can be fabricated with any thickness ranging between 500 and 50 μm. Devices with thinner cross sections, 20 μm, have been made using silicon on insulator (SOI) wafers.

Following the completion of the backside etch process, a 500-nm-thick PECVD silicon dioxide film is deposited over the backside of the wafer. This film acts as an etch stop when patterning the remaining 100 μm of silicon on the front of the wafer. The film prevents the deposition of the fluorocarbon Bosch polymers on the backside of the wafer during the final DRIE etch.

Patterning the front side of the wafer is a four-step process. First, the silicon dioxide film used to seal the via holes and the silicon nitride channel structure are patterned by RIE, defining the profile of the device. A photoresist mask with the device profile and outlet ports is then aligned and patterned directly on the silicon dioxide hard mask. A DRIE process is used to etch through the exposed silicon to the deposited etch stop. An RIE process is then used to remove the silicon dioxide etch stop and open the fluid inlet and outlet ports. Waiting to open the outlet ports until all of the DRIE processes are complete is important because it prevents any residue from the hydrophobic Bosch fluorocarbon polymer from depositing inside the channel, making the channels easier to fill.

The completed device has a shank that is 2 mm long, matching the approximate thickness of the rat premotor cortex. [Fig. 2(a)] The cross section of the shaft is 120 μm wide and 100 μm thick. The shank width was increased slightly compared to the first-generation nonfluidic devices in order to adjust the orientation of the fluid outlet ports. The shank thickness of 100 μm was maintained so that future biocompatibility studies could be compared with previous studies conducted using 100 μm $\times$ 100 μm cross section probes. It is important to emphasize again that this process is extremely flexible allowing probe dimensions be varied to suit different research or clinical goals. Like the first-generation probes the handle of the device is a 500-μm cube [Fig. 2(a)], thus permitting devices to be consistently aligned and inserted using our automated insertion device.

A fluidic interconnect used to attach the model probe to a glass capillary or Tygon MicroBore Tubing © (Smallparts Inc., Miami Lakes, FL) has a 100 μm $\times$ 100 μm cross section and is aligned with the axis of the device shaft. It protrudes 1.5 mm from the handle of the device. The microchannel inlet is centered at the end of the interconnect. The length of the interconnect helps prevent clogging when the device is sealed to the fluid reservoir. Four pairs of channel outlets are spaced at 500-μm intervals along the device shank. The outlets are 30×15 μm [Fig. 2(c)]. The number and size of the outlet ports can be varied to achieve different drug release rates and concentration profiles based on the desired outcome.

B. Assessment of Reactive Cell and Tissue Responses

Immunohistochemical analysis of serial 100-μm-thick slices of adult male rat brains were performed at 1 h, 24 h, and 6 weeks post insertion in order to define the extent of the reactive response in neural tissue surrounding first-generation model silicon probes. At the desired time points, animals were perfusion fixed with 4% paraformaldehyde. The brain was dissected with the implanted devices in place, and block fixed. Devices were then removed and brains were sectioned into 100-μm-thick slices perpendicular to the device shank orientation. Tissue slices were washed, blocked with goat serum 0.2% triton X-100 in HEPES-Hanks' saline for 1 h, and incubated for 72 h in the primary monoclonal antibodies for phospho-SAPK/JNK G9 (Cell Signaling, #9255) (1:500), diluted in 2% goat serum, 0.1% triton X-100 in HEPES-Hanks' saline at 4 °C. The tissue slices were washed and incubated overnight at 4 °C with secondary antibody goat anti-mouse Alexa Fluor 488 (1:200) and NeuroTrace for Nissl staining (1:100) (Molecular Probes, Eugene, OR). Processed slices were washed and mounted in a glycerol solution containing n-propyl gallate to reduce photo bleaching. Samples were viewed with an inverted fluorescent microscope (Olympus America Inc., Melville, NY) and imaged using a confocal laser scanning attachment (Prairie Technologies Inc., Middleton WI).

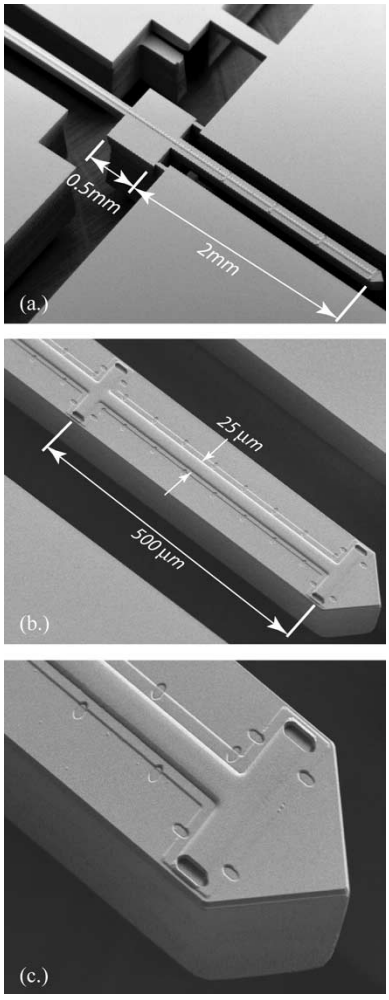

Fig. 2. Scanning Electron Microscope (SEM) images of model silicon prostheses with integrated microchannels were taken at (a) 25 $\times$ (b) 200 $\times$ (c) 500 $\times$.

C. In Vitro Studies: Release Into Agarose Phantoms

Time lapse images of Texas Red labeled transferrin (TR-transferrin, 80 kD) and dextran (TR-dextran, 3 kD)

(Molecular Probes, Eugene, OR) being released from the device microchannels and diffusing into agarose brain phantoms were collected and analyzed. Probes were fixed to glass capillary tubing using a two-component epoxy adhesive (Miller Stephenson Chemical Company Inc., Danbury, CT). The assembly was allowed to cure for 24 h. Each assembly was back-filled with either a 1 g/mL solution of TR-transferrin or a 10 mg/mL solution of TR-dextran in buffered saline (pH 7.3) using a 34-gauge MicroFil syringe (World Precision Instruments, Sarasota, FL). The assembly was attached to a micro-manipulator and inspected under an epifluorescent microscope (Olympus America Inc., Melville, NY) to insure that the fluidic channels were structurally intact, completely filled, and free of fouling or air bubbles.

Agarose [1% (w/v)] was cut into $5 \times 5 \times 3$ mm blocks and set on glass microscope slides. Once the agarose was positioned in the field of view of an epifluorescent microscope, devices were inserted channel side up into the side of the agarose block. Time-lapse images were digitally recorded using a charge-coupled device camera (The Cooke Corporation, Auburn Hills, MI.) and digital imaging software (Image Pro Plus, Media Cybernetics, Carlsbad, CA). Fluorescence intensity line profiles were extracted from the acquired images and compared with fluorescence distributions predicted by analytical solutions of the diffusion equation.

D. In Vivo Experiments: Release Into Rat Brain Cortex

Devices were fixed to PVC-tygon tubing. The tubes were cut to a length of 1.5 cm and backfilled with a 5 mg/mL TR-transferrin solution in buffered saline (pH 7.3) in the same manner as described above. Adult male Sprague–Dawley rats were anesthetized with a 4:1 solution of Xyla-Ject (Xylazine)/Ketamine mix (0.625 ml/1.0 ml) and Hepes- Hanks' saline. Device insertion and surgical methods were similar to those previously described [9], [10], [12]–[14]. An incision was made along the midline of the skull and tissue was carefully pulled aside. Holes were drilled in the skull at two insertion sites located approximately 1 mm from midline and 2 mm caudal from bregma (Fig. 3). Care was taken to locate the insertion sites in areas devoid of large blood vessels. Devices were inserted and left in animals for 30 min, 1h, and 5 h. Animals were kept anesthetized for the duration of the experiment. At the specified times, animals were perfusion fixed using a 4% paraformaldehyde solution. Brains were removed, blocked, and cut into 100-μm thick tissue slices parallel to the device shank orientation using a vibratome (FHC, Bowdinham ME). Tissue slices were mounted in chambers made on slides containing mounting media (95% glycerol, 5% MBMS, n-propyl-gallate) and imaged using a scanning confocal system mounted on an inverted microscope. The 3-D data sets for each tissue slice were aligned and superimposed using Adobe Photoshop and presented as through focus projections, (Fig. 4).

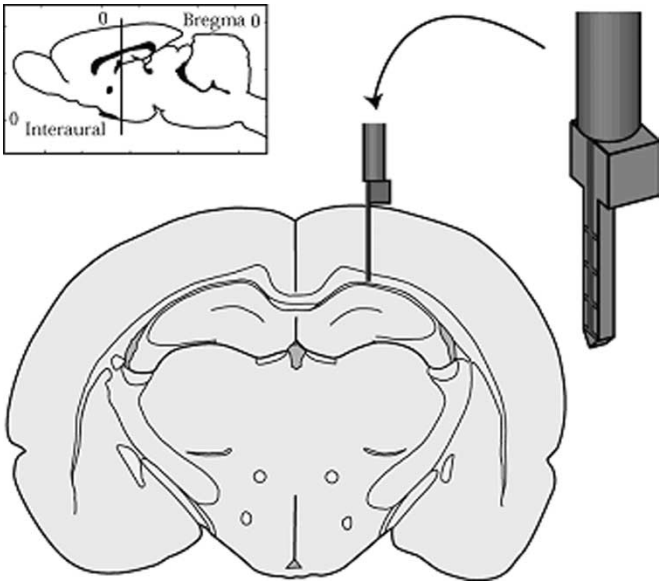

Fig. 3. Devices were oriented so that the microfluidic channels faced medially. Microfluidic devices were inserted 3 mm caudal from Bregma and roughly 2 mm lateral to the midline.

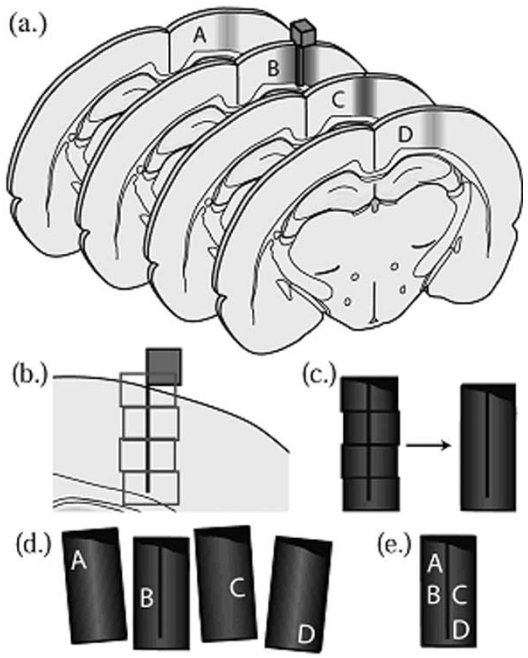

Fig. 4. (a) A series of consecutive 100 μm-thick coronal tissue slices were cut parallel to the device shaft. The position of an inserted device is illustrated in section B. (b) A series of overlapping confocal images were collected along the entire length of the inserted device. (c) These confocal images were aligned and merged to produce a composite image of each tissue slice. (d) Composite images from each tissue slice were rendered partially transparent to give each equal weight (e) then placed in register according to the insertion site and the surface of the cerebrum, to produce a through focus projection of the affected tissue volume.

VI. Results and Discussion

A. Device Design and Fabrication

In addition to creating a model silicon probe with fluidic channels, additional experimental constraints guided the fabrication of the fluidic devices used in this study. Specifically, the fluidic probes needed to retain the geometry of the first-generation model probes. In order to retain the shank thickness and cubic handle geometry, double-sided DRIE processing was used in the fabrication of the fluidic devices just as it was used for the first-generation model probes. This meant that extreme care

needed to be taken when handling samplings in order to prevent fouling or shattering of the wafer during processing. Also, because the DRIE/Bosch etch process relies on the deposition of a fluorocarbon polymer to maintain anisotropy, process steps needed to be carefully ordered so that none of the hydrophobic polymer was deposited inside fluidic channels or on the backside of the device.

The use of surface micromachining techniques for the formation of the fluidic channels affords a great deal of flexibility in both channel geometry and materials. Different sacrificial and structural materials can be utilized to define the hydraulic diameter and form the channel walls so long as those materials are compatible with subsequent fabrication techniques. Alternative sacrificial materials include thermally degrading polymers, metals, and photoresist. Possible structural film alternatives include polysilicon, silicon dioxide, polyimide, or parylene. Different materials can be chosen to accommodate various surface modification strategies or to explore how different materials affect the reactive response. In addition to material variations, wet etching steps can be integrated into the fabrication process to increase the channel cross-section. Using potassium hydroxide to etch into the bulk silicon after the channel structure is formed, but before the channel is sealed, it is possible to significantly increase the height of the channel to better accommodate active pumping and increase channel volume. Overall, the fabrication process developed for the current generation devices retains the geometry used in ongoing biocompatibility studies, while still affording the flexibility to change materials, adapt new delivery strategies, and ultimately incorporate thin film electrodes for recording and stimulation.

B. MAPK Immunohistochemistry

The subfamily SAPK/JNK was selected as a sensitive indicator of cell stress and activation to enable a qualitative estimate of the tissue region affected by device insertion. Time points at 1 h, 24 h, and 6 weeks following device insertion were investigated to establish the extent of the reactive tissue region, or zone of influence. Results from immunohistochemistry showed time-dependent changes of MAPK activation following device insertion [Fig. 5(c)]. At 1 h postinsertion SAPK/JNK activation was observed within a 600-μm radius of the implantation site. An increase in activated phosphorylated SAPK/JNK was seen over time and extended approximately 800 μm from the probe site at 24 h. The 6-week time point showed a tighter band of cellular activation for SAPK/JNK, extending only 400 μm from the insertion site [Fig. 5(d)]. No activation was observed in tissue slices where no device was inserted [Fig. 5(a)].

C. In Vitro Studies: Molecular Release Into Agarose Phantoms

Observations of the release of TR-transferrin and TR-dextran in agarose brain phantoms were used to establish standard procedures for filling, insertion, and measurement of diffusion characteristics. Prior to insertion, devices were examined to insure that channels were free of debris and air bubbles. Air bubbles and small air gaps were common following filling. However, over periods of a few minutes, these air gaps and bubbles were adsorbed into the solution and were not a factor during

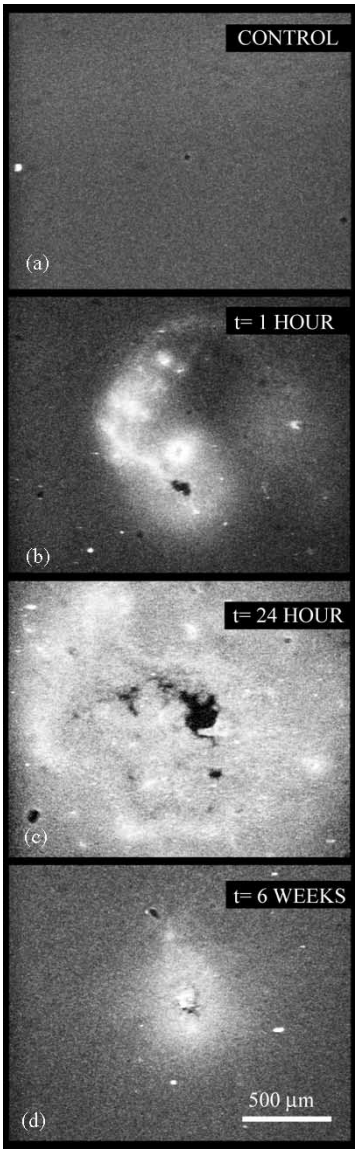

Fig. 5. (a) No SAPK/JNK activation is observed without device insertion. (b) Activation of MAPK SAPK/JNK pathway was observed at (b) 1 h, (c) 24 h, and (d) 6 weeks following device insertion.

insertions. The small cross section of the channels made viscous losses associated with even very low flow rates extremely high. Consequently pressure driven flow was not used to clear the channels of bubbles or air gaps.

In order to minimize tearing of the agarose phantoms and avoid the production of low-resistance flow paths along the device shank, devices were carefully aligned with the axis of motion during insertions. As devices were inserted into the agarose phantoms, the labeled compounds were observed to quickly diffuse into the agarose along the insertion path. This resulted in higher fluorescence intensities near the point where the probe first penetrates the agarose surface [Fig. 6(a)]. Release profiles within 10 min of device insertions varied from one insertion to the next due to variations in outlet port function. Because these variations were observed during insertions performed with different devices and repeated insertions of the same device, they were likely produced by blockages of the outlets caused by small pieces of agarose or other particulates

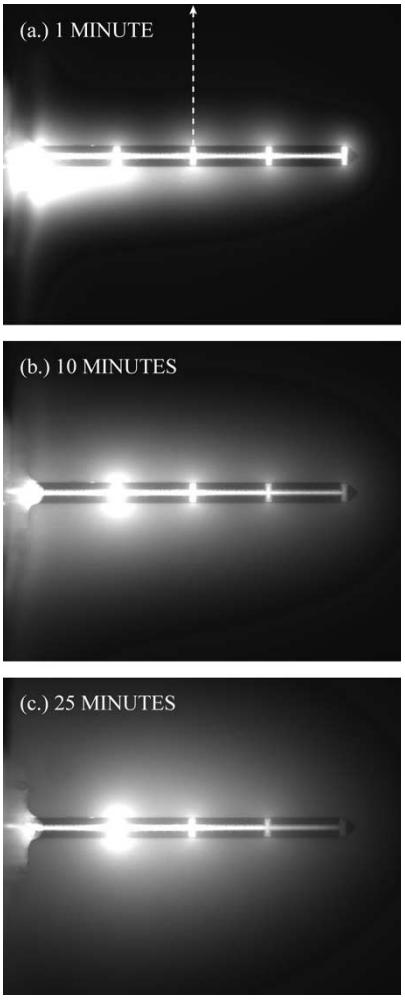

Fig. 6. Release of 10 mg/mL TR-Dextran into agarose phantoms at (a) 1, (b) 10, and (c) 25 min. Images were recorded at 10 second intervals over a 30-min period using an epifluorescent microscope equipped with digital imaging equipment.

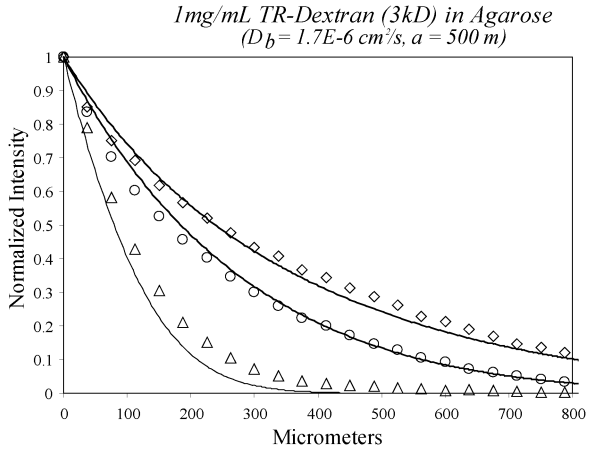

Fig. 7. Intensity line profiles taken from images Fig. 5(a)–(c) [as indicated by a dashed line in Fig. 5(a)] show a decay in fluorescence intensity, and corresponding concentration, moving away from the probe shank. This type of decay is to be expected from diffusion mediated transport. Solid lines represent theoretical predictions for profiles based on $a = 500\ \mu\mathrm{m}$, and $D_b = 1.7E-6\ \mathrm{cm}^2/\mathrm{s}$.

that fouled the openings during handling. It is possible that similar fouling problems could alter performance *in vivo*. Within 10 min after the insertion, fluorescence intensity profiles from different insertion events were more consistent due to the continued diffusion of material into areas of low concentration.

Shortly following insertion, intensity profiles taken from representative images shown in Fig. 6 are consistent with profiles predicted for the diffusion of molecules from a source of constant concentration (Fig. 7). As mentioned previously, the theoretical model is adjusted to account for the quasispherical diffusion taking place at the outlet port by setting $a = 500\ \mu$m. More rigorous justification for the choice of a could be accomplished using finite element analysis. Nonetheless Fig. 7 verifies that transport of molecules from the microchannels is strictly mediated by diffusion.

Within 15 min of implantation, a recognizable intensity gradient (corresponding to a concentration gradient) developed inside the channels. The intensity was highest near the reservoir and rapidly decreased toward the tip of the device. This gradient progressed to a steady-state of low fluorescence intensity in the channels. No observable change in fluorescence intensity, e.g., flux of solute from the outlet ports, was evident near the tip of the device once this gradient was established. These results indicate that the current device configuration will allow rapid drug or biochemical release but delivered drug concentrations could become very low at longer time points. If these concentrations were sufficiently below the K_d for drug-receptor interactions, the drugs would have little biological effect.

Circulating flow through the channels would eliminate this problem and allow for chronic passive delivery. Additionally, increasing the volume, of the channels, would extend periods of efficient diffusion-mediated drug delivery and facilitate active convective delivery. New model probes with increased channel volumes that incorporate novel evaporative pumping mechanisms to induce circulation of fluid within the channels are currently being developed.

It is clear that the steady-state conditions realized in brain tissue will be significantly different from that observed in agarose brain phantoms because the model phantoms do not exhibit any of the variations in permeability, vascular perfusion, receptors, transporters or elimination characteristic of the brain. However these experiments provide a basic understanding of device function, and give direction for the development of the next generation of microchannel devices. These results also suggest that a coupled theoretical model for diffusion within the microchannels into the agarose volume could provide a better model of device performance.

D. In Vivo Experiments: Release Into Rat Brain Cortex

Transferrin is not a candidate for intervention pharmacology; however, it has a number of attributes that make it an ideal test biomolecule for assessing the functionality of the model probes: 1) it is concentrated in neurons by receptor-mediated endocytosis [23]; 2) its size, $\sim 74\,000$ daltons, is similar to cytokines, growth factors, and hormones being considered for intervention; and 3) it is available labeled with a variety of fluorophores allowing it to be used in multispectral imaging studies. Most importantly transferrin is readily taken up by neurons and becomes sequestered within cells, it is not washed away during perfu-

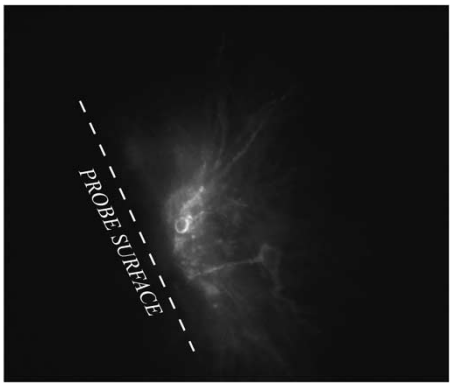

Fig. 8. Both highly localized and diffuse fluorescence from TR-transferrin was observed at high magnifications (50 ×). Localized fluorescence was clearly directed by cellular uptake along cell bodies and dendritic processes.

sion fixation, thus allowing us to more accurately describe its distribution. Because transferrin has a relatively large hydraulic radius, and lower diffusivity than small molecule pharmaceuticals such as dexamethazone, it provides a conservative estimate of the affected tissue volume.

Following insertions TR-transferrin diffused into nearby neural tissue from the microchannel outlets at the earliest times studied. No significant variations in fluorescence intensity or distribution were observed at later times.

Fluorescence signals were observed as both diffuse and localized staining. The diffuse staining represents TR-transferrin cross-linked to proteins in the extracellular space. Localized staining was observed in neuronal cell bodies and dendritic processes (Fig. 8). At 30 min postinsertion the TR-transferrin intensity profile had a steep gradient with significant fluorescence signal observed as far as 400 μm from the insertion site [Fig. 9(c) and (d)]. Based on diffusion lengths predicted by the steady-state model of diffusion coupled with first-order elimination of solute in the tissue volume (Fig. 10), it is reasonable to assume that the system had reached a steady-state at the 30-min time point. Values for the apparent diffusivity and elimination of Transferrin were estimated based on values for similarly sized molecules. Future studies that strictly analyze the performance of these devices will require the verification of these values using independent methods.

As mentioned, the lack of variation between the 30-min, 1-h, and 5-h insertions is consistent with the observation that the system had reached a nearly steady-state within 30 min. It is also consistent with results of the *in vitro* studies. Because it is unlikely that significant additional TR-transferrin was delivered after 30 min and the metabolism of Texas Red fluorescent molecules captured inside cells is relatively slow, it is reasonable to expect little change in fluorescence beyond the 30-min time point.

Although these results indicate the early reactive response (measured at 1 h and 24 h) extends slightly beyond the tissue zone affected by diffusion-mediated transport of TR-transferrin, the volume of tissue exhibiting long-term reactive activity is comparable to the volume addressed by release from the microchannels. Since the effectors of the early responses are released immediately around implanted devices, early release of therapeutics into the tissue within a few hundred micrometers of

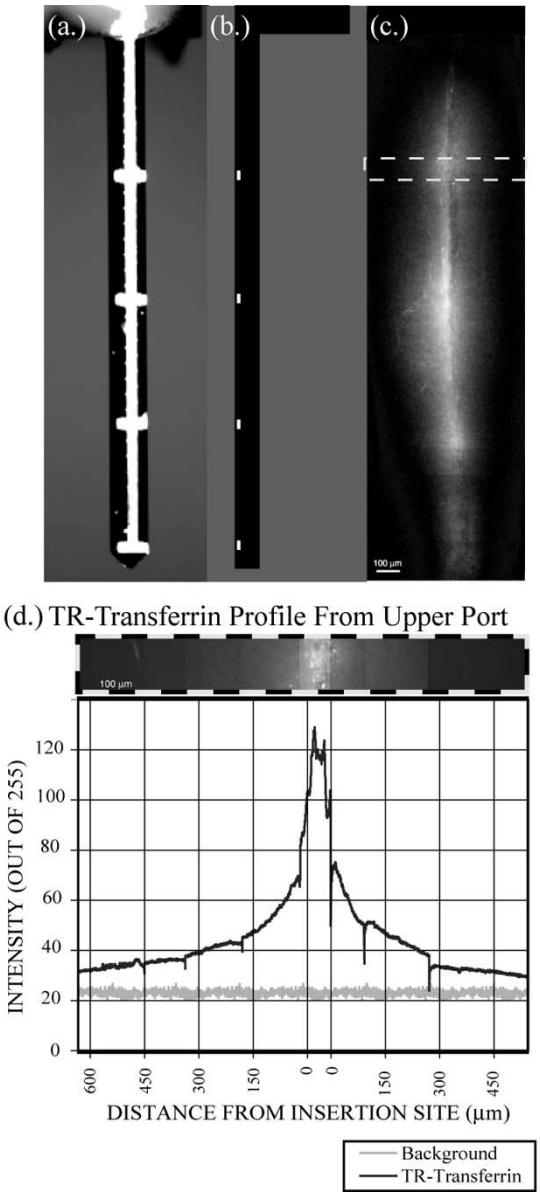

Fig. 9. (a) Scale top-view image of a device and corresponding (b) side-view orientation of the device relative to (c). (c) A composite image prepared using 10 × confocal images taken from 6 tissue slices. (d) An intensity profile taken from the region of (c) outlined by the dashed line. A horizontal series of 40 × images were collected along the upper port within the boxed region. A composite image was produced (upper figure, part (d)). A similar background image was prepared by collecting images from a similar region of cortex distant to the insertion site.

the device immediately following insertion may limit the extent of the early response. Thus, diffusion-based delivery may effectively control release of signaling molecules responsible for the cascading cell-to-cell signaling that contributes to the larger zone of influence described by SAPK/JNK activation at 24 h.

VII. Conclusion

This paper demonstrates the successful fabrication of silicon-based model cortical probes with integrated microchannels that can be used to alter the biochemical composition of tissue around implanted devices. This presents a unique potential approach for controlling the reactive response of neural

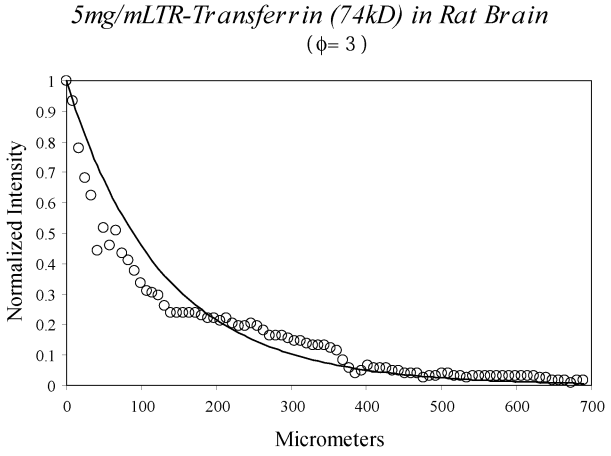

Fig. 10. The intensity profile from Fig. 9(d) as compared to the theoretical steady-state model of diffusion from a constant spherical source. ϕ (Thiele modulus) $= 3$.

tissue to chronically implanted multielectrode arrays. Devices were characterized *in vitro* using agarose brain phantoms and time lapse imaging to characterize the release of fluorescently labeled transferrin and dextran molecules from the microchannels into the surrounding porous media. Real time observations of device release provided insight into device performance that was not available from *in vivo* experiments. *In vivo* experiments demonstrated the feasibility of delivering biologically active proteins into a volume of tissue that is comparable in size to the zone of influence described by SAPK/JNK activation following device insertion. Because the reactive responses develop over a relatively long time scale, drug delivery by diffusion without the need for pumps and valves is a practical solution. This paper represents preliminary steps toward developing a viable clinical intervention strategy to improve the biocompatibility and long-term stability of implantable silicon-based multielectrode arrays to be used for the treatment of neurological damage associated with trauma and disease.

ACKNOWLEDGMENT

The authors would like to acknowledge the Cornell Nanofabrication Facility, supported by the National Science Foundation, for fabrication work and scanning electron microscopy. Flourescent images taken *in vitro* were collected using the W. M. Keck Foundation High Speed Flow Visualization System.

REFERENCES

[1] T. M. Vaughn, W. J. Heetderks, L. J. Trejo, W. Z. Rymer, M. Weinrich, M. M. Moore, A. Kubler, B. H. Dobkin, N. Birbaumer, E. Donchin, E. W. Wolpaw, and J. R. Wolpaw, "Guest editorial: Brain-computer interface technology: A review of the second international meeting," *IEEE Trans. Rehab. Eng.*, vol. 11, pp. 94–109, June 2003.

[2] Q. Bai and K. D. Wise, "Single unit neural recording with acute microelectrode arrays," *IEEE Trans. Biomed. Eng.*, vol. 48, pp. 911–920, Aug. 2001.

[3] P. J. Rousche and R. A. Normann, "Chronic intracortical microstimulation (ICMS) of cat sensory cortex using the utah incortical electrode array," *IEEE Trans. Rehab. Eng.*, vol. 7, pp. 56–68, Mar. 1999.

[4] K. L. Drake, K. D. Wise, J. Farraye, D. J. Anderson, and S. L. BeMent, "Performance of planar multisite microprobes in recording extracellular single-unit intracortical activity," *IEEE Trans. Biomed. Eng.*, vol. BME-35, pp. 719–732, Sept. 1988.

[5] P. J. Rousche, D. S. Pellinen, D. P. Pivin, J. C. Williams, R. J. Vetter, and D. R. Kipke, "Flexible polyimide-based intracortical electrode arrays with bioactive compatability," *IEEE Trans. Biomed. Eng.*, vol. 48, pp. 361–371, Mar. 2001.

[6] D. T. Kewley, M. D. Hills, D. A. Borholder, I. E. Opris, N. I. Maluf, C. W. Storment, J. M. Bower, and G. T. A. Kovacs, "Plasma etched neural probes," *Sens. Actuators*, vol. A 58, no. 27, 1997.

[7] J. J. Burmeister, K. A. Moxon, and G. A. Gerhardt, "Ceramic-based multisite microelectrodes for electrochemical recordings," *Analytical Chem.*, vol. 72, no. 1, pp. 187–192, 2000.

[8] D. R. Kipke, R. J. Vetter, J. C. Williams, and J. F. Hetke, "Silicon-substrate intracortical microelectrode arrays for long-term recording of neuronal spike activity in cerebral cortex," *IEEE Trans. Rehab. Eng.*, vol. 11, pp. 151–154, June 2003.

[9] J. N. Turner, W. Shain, D. H. Szarowski, M. D. Andersen, S. Martins, M. Isaacson, and H. G. Craighead, "Cerebral astrocyte response to micromachined silicon implants," *Exp. Neurol.*, vol. 156, pp. 33–49, 1999.

[10] D. H. Szarowski, M. D. Andersen, S. Retterer, A. J. Spence, M. Isaacson, H. G. Craighead, J. N. Turner, and W. Shain, "Brain responses to micromachined silicon devices," *Brain Res.*, vol. 983, no. 1–2, pp. 23–35, Sept. 2003.

[11] D. J. Edell, V. V. Toi, V. M. McNeil, and L. D. Clark, "Factors influencing the biocompatibility of insertable silicon microshafts in cerebral cortex," *IEEE Trans. Biomed. Eng.*, vol. 39, pp. 635–643, June 1992.

[12] L. Spataro, J. Dilgen, S. Retterer, A. Spence, M. Isaacson, J. Turner, and W. Shain, "Dexamethasone treatment reduces astroglia responses to inserted neuroprosthetic devices in rat neocortex," J. Neurosci., submitted for publication.

[13] W. Shain, L. Spataro, K. Haberstraw, J. Dilgen, S. Retterer, A. Spence, M. Isaacson, and J. Turner, "Controlling cellular reactive responses around neural prosthetic devices using peripheral and local intervention strategies," *IEEE Trans. Rehab. Eng.*, vol. 11, pp. 186–188, June 2003.

[14] K. L. Smith, A. E. Anderson, D. J. Spataro, J. Dilgen, and W. Shain, "Modulation of MAPK pathways following insertion of prosthetic devices. Presented at neuroscience 2002," presented at the Society for Neuroscience 32nd Annu. Meeting, Orlando, FL, 2002.

[15] J. Chen, K. D. Wise, J. Hetke, and S. Bledsoe, "A multichannel neural probe for selective chemical delivery at the cellular level," *IEEE Trans. Biomed. Eng.*, vol. 44, pp. 760–769, Aug. 1997.

[16] R. Rathnasingham, D. R. Kipke, S. C. Bledsoe Jr, and J. D. McLaren, "Characterization of implantable microfabricated fluid delivery devices," *IEEE Trans. Biomed. Eng.*, vol. 51, pp. 138–145, Jan. 2004.

[17] D. Papargeorgiou, S. C. Bledsoe, M. Gulari, J. F. Hetke, D. J. Anderson, and K. D. Wise, "A shuttered probe with in-line flowmeters for chronic in-vivo drug delivery," in *Proc. 14th IEEE Int. Conf. Micro Electro Mechanical Systems, 2001 (MEMS 2001)* , 2001, pp. 212–215.

[18] W. M. Saltzman and M. L. Radomsky, "Drugs released from polymers: Diffusion and elimination in brain tissue," *Chemical Engineering Science*, vol. 46, no. 10, pp. 2429–2444, 1991.

[19] C. H. Mastrangelo, J. H.-J. Yeh, and R. S. Miller, "Electrical and optical properties of vacuum-sealed polysilicon microlamps," *IEEE Trans. Elec. Dev.*, vol. 39, pp. 1363–1375, June 1992.

[20] L. Lin and A. P. Pisano, "Silicon-processed microneedles," *IEEE J. MEMS*, vol. 8, pp. 78–83, March 1999.

[21] "Laermer F and Schilp A 1996 Method of Anisotropically Etching Silicon," US Patent 5 501 893.

[22] H. Ichijo, E. Nishida, K. Irie, P. Dijke, M. Saitoh, T. Moriguchi, M. Takagi, K. Matsumoto, K. Miyazono, and Y. Gotoh, "Induction of apoptosis by ASK1, a mammalian MAPKKK that activates SAPK/JNK and signaling pathways," *Science*, vol. 275, no. 5296, pp. 90–94, Jan. 1997.

[23] T. Moos and E. H. Morgan, "Transferrin and transferrin receptor function in brain barrier systems," *Cellular Molecular Neurobiol.*, vol. 20, no. 1, pp. 77–95, 2000.

Scott T. Retterer received the B.S. in mechanical engineering from the University of Illinois at Chicago, Chicago, IL, in 2000. He has been a Keck foundation fellow, and is currently an NSF predoctoral fellow working toward the Ph.D. degree in biomedical engineering at Cornell University, Ithaca, NY.

His research interests are in the areas of therapeutic and diagnostic microdevices, biocompatibility of implantable bioMEMs, and microfabricated systems for rare cell isolation and characterization.

Karen L. Smith received the B.S. degree in environmental studies from Springfield College, Springfield, MA, in 1980, and the M.S. degree in biology from the State University of New York at Albany, Albany, NY, in 1997.

She is currently a Research Scientist in the Laboratory of Nervous Disorders at the Wadsworth Center, New York State Department of Health, Albany, NY. Her research interests include the simultaneous visualization and recording from individual neurons, and the development of immunohistochemical procedures and biochemical assays for examining the reactive cell and tissue responses to implantable devices.

Christopher S. Bjornsson received the B.Sc. degree in genetics and the Ph.D. degree in developmental cell biology from the University of Manitoba, Winnipeg, MB, Canada, in 1995 and 2003, respectively.

He is a Postdoctoral Investigator at the Wadsworth Center, New York State Department of Health, Albany, NY. His research is focused on describing neurovascular responses to neural prosthetic devices, and evaluating the efficacy of local drug delivery in treating the reactive responses to these devices.

Dr. Bjornsson has received Canadian NSERC Postgraduate Scholarships, as well as departmental and faculty awards from the University of Manitoba for excellence in teaching. He is a member of the Societies for Neuroscience and Cell Biology, and has regularly presented his work at national meetings.

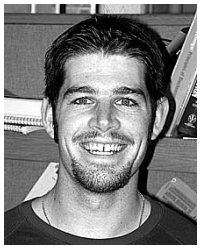

Keith B. Neeves received the B.S. degree in chemical engineering from the University of Colorado at Boulder in 2000. He is working towards the Ph.D. degree in the School of Chemical and Biomolecular Engineering at Cornell University, Ithaca, NY.

He is an Epilepsy Foundation Fellow. His research is focused on developing smart drug delivery devices for the treatment of neurological disorders and modeling transport in biological tissues.

Mr. Neeves has received fellowships from NSF, the Keck Foundation, and the Epilepsy Foundation of America.

Andrew J. H. Spence was born in Oxford, U.K., in 1975. He received the B.S. degree in physics from the University of California at Berkeley, Berkeley, CA, in 1997, and the Ph.D. degree in applied and engineering physics from Cornell University, Ithaca, NY, in 2003.

His research interests are in the areas of microfabricated devices for neural recording, neural ensemble coding, invertebrate sensory systems and behavior, and signal processing and electronic design.

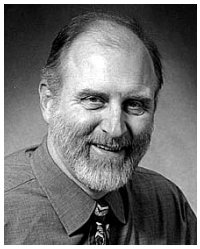

James N. Turner received the B.S. degree in engineering science and the Ph.D. degree in biophysics from the State University of New York at Buffalo, in 1968 and 1973, respectively. He did National Institutes of Health and National Science Foundation Postdoctoral Fellowships at the Roswell Park Memorial Institute, Buffalo.

Currently, he is Director of the Three-Dimensional Light Microscopy Facility and the Nanobiotechnology Program at the Wadsworth Center of the New York State Department of Health, Albany and a Platform Leader and Executive Committee Member of the Nanobiotechnology Center, an NSF sponsored Science and Technology Center lead by Cornell University. He is a Professor of Biomedical Engineering at Rensselaer Polytechnic Institute, Troy, NY, and Biomedical Sciences in the School of Public Health of the University at Albany. He is interested in applications of light imaging methods and quantitative image analysis in biology and medicine with a specific emphasis on the nervous system. He is on the editorial board of *Microscopy and Microanalysis* and IEEE TRANSACTIONS ON NANOTECHNOLOGY.

Dr. Turner has chaired numerous symposia in the area of 3-D microscopy, both light and electron, at national meetings. He is a member of the Microscopy Society of America, International Society for Analytical Cytology, and the Society for Neuroscience. He frequently serves on NIH advisory panels.

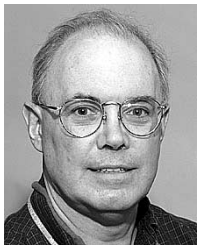

William Shain received the B.A. degree in biology from Amherst College, Amherst, MA, in 1966 and the Ph.D. degree in developmental/cell biology from Temple University, Philadelphia, PA, in 1972.

He was a postdoctoral fellow in neurobiology in Marshall Nirenberg's laboratory at the National Institutes of Health for three years. Currently, he is a Research Scientist at the Wadsworth Center and Associate Professor in the Department of Biomedical Sciences, School of Public Health, University at Albany. His laboratory uses micro- and nano-fabricated devices for the study of brain and brain cell function. He is Director of a Bioengineering Research Partnership from NIBIB to study tissue integration of neural prosthetic devices and is Project leader in the Nanobiotechnology Center, a NSF-sponsored Science and Technology Center lead by Cornell University.

Dr. Shain is a member of the Societies for Neuroscience, Neurochemistry, Cell Biology, and Biomaterials. He frequently serves on NIH advisory panels.

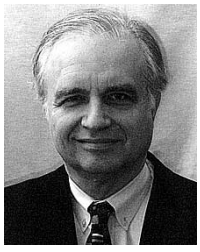

Michael S. Isaacson (M'03) received the B.S. degree in engineering physics from the University of Illinois at Urbana-Champaign and the Ph.D. in physics from the University of Chicago, Chicago, IL.

He has been on the scientific staff in the Division of Biology at Brookhaven National Laboratory and a member of the faculty of the Physics Department at the University of Chicago and the School of Applied and Engineering Physics at Cornell University (Ithaca, NY) before moving to University of California at Santa Cruz. His research interests include the development of novel nanocharacterization tools using electron and photon optics and the fabrication of nano/microdevices for biomedical applications.

Dr. Isaacson has been President of the Microscopy Society of America and is currently Secretary/Treasurer of the Engineering Research Council of the ASEE. In addition, he is a fellow of the AAAS. Among numerous awards are an Alexander von Humboldt Senior Scientist award, the Burton Medal from the Microscopy Society of America and the Rank Prize in Optoelectronics. He is currently Prof. Emeritus in the School of Applied and Engineering Physics at Cornell University and the Narinder Singh Kapany Professor of Optoelectronics at the University of California at Santa Cruz.